SUPPLEMENTAL FIGURES

Figure S1, related to Figure 1

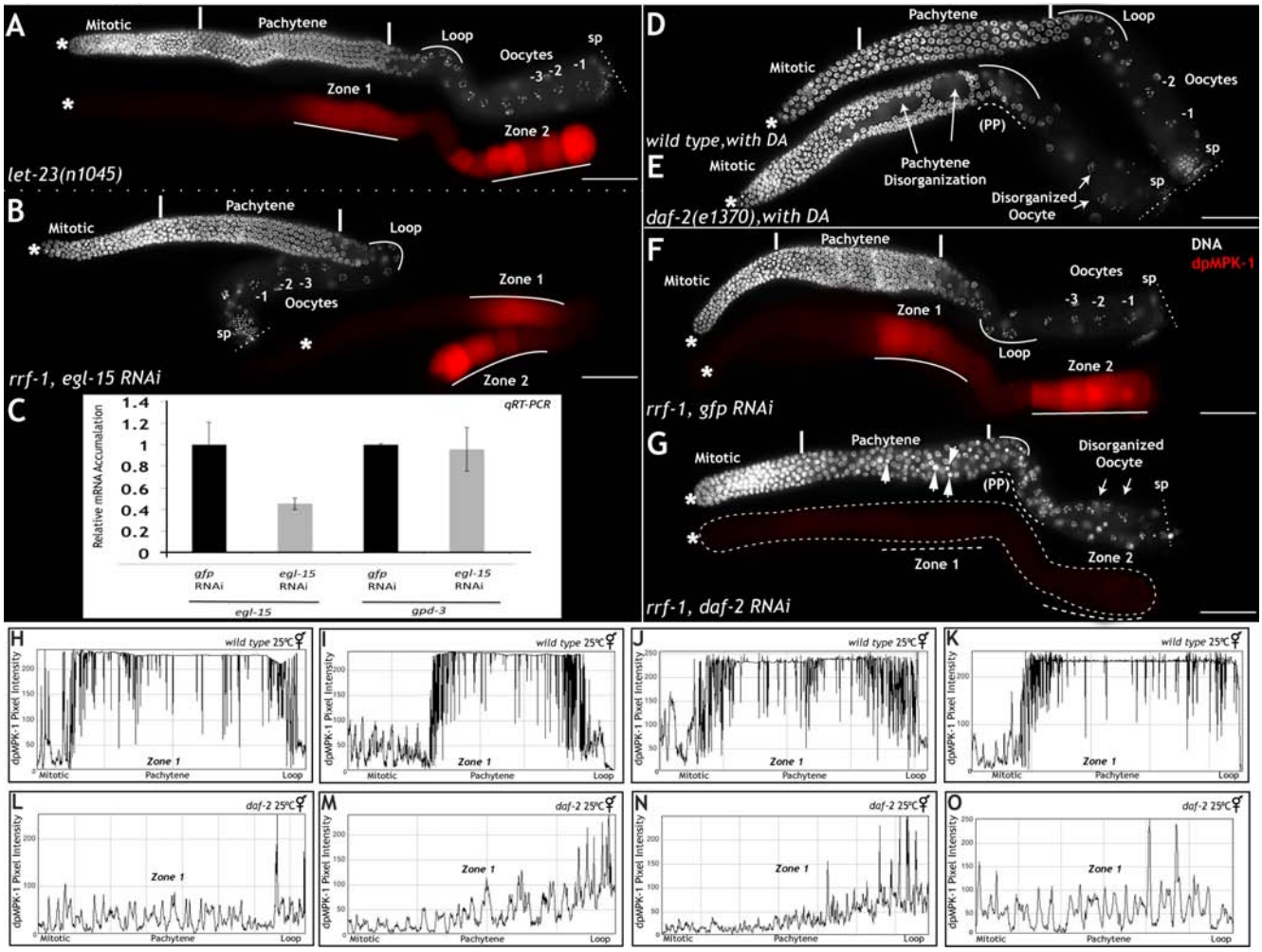

Figure S2, related to Figure 2

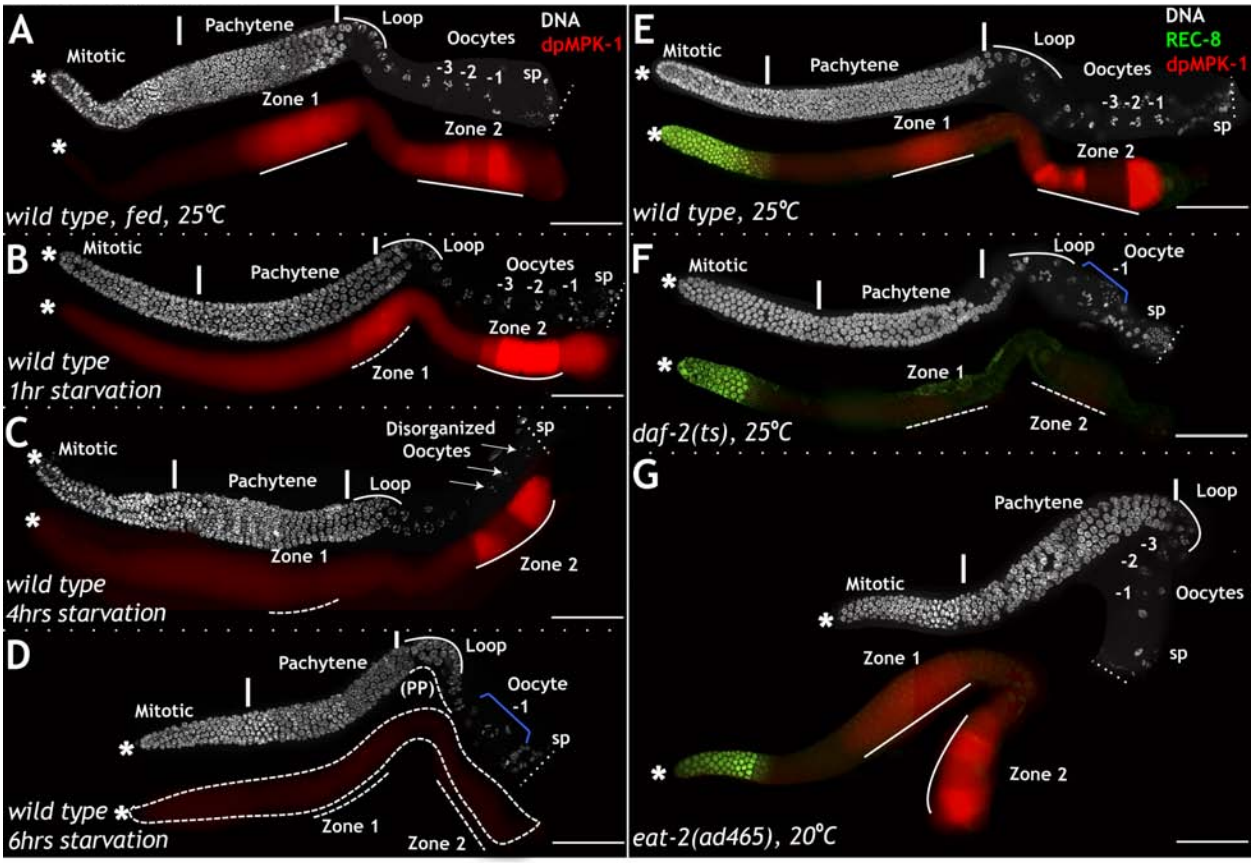

Figure S3, related to Figure 3

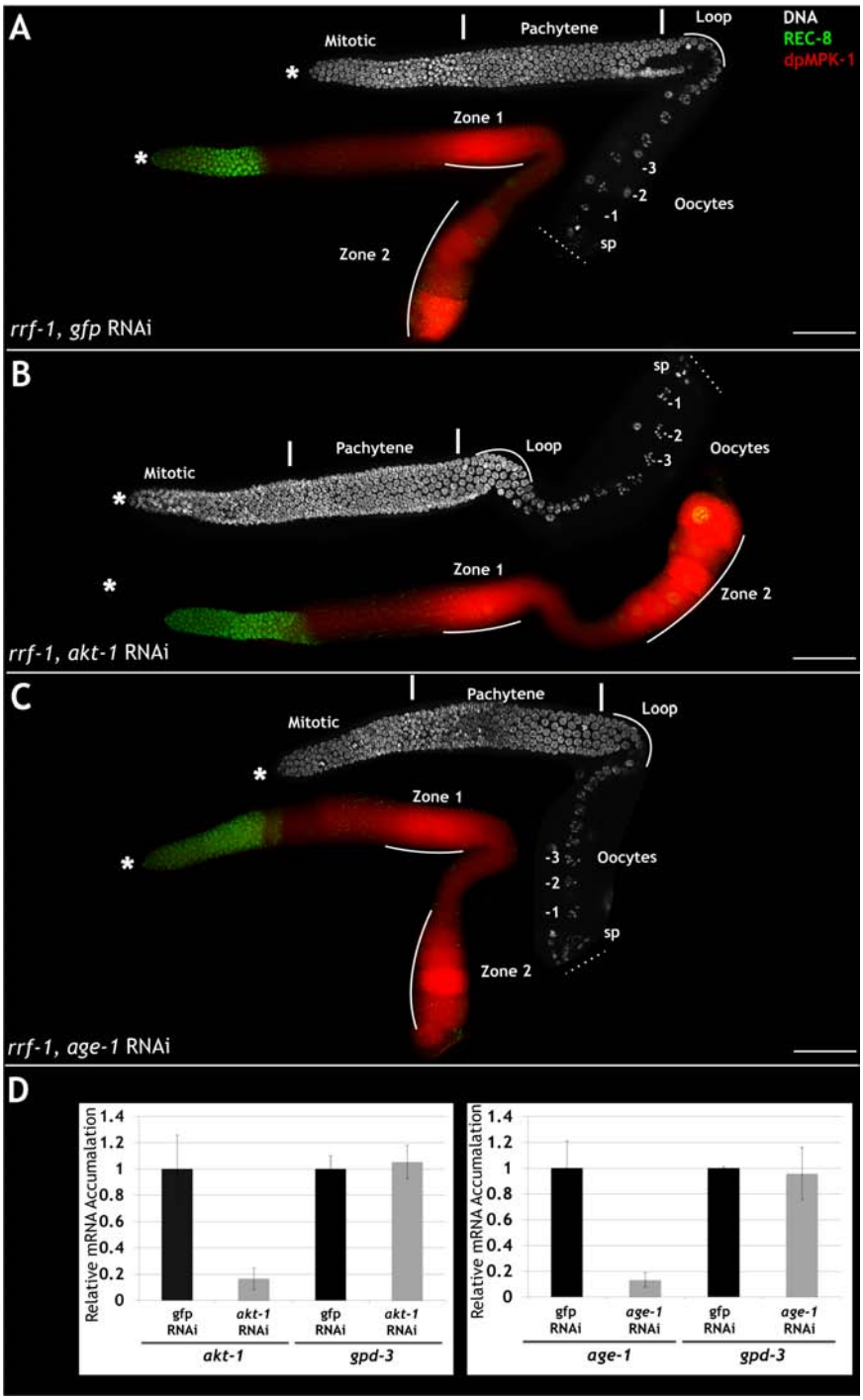

Figure S4, related to Figure 4

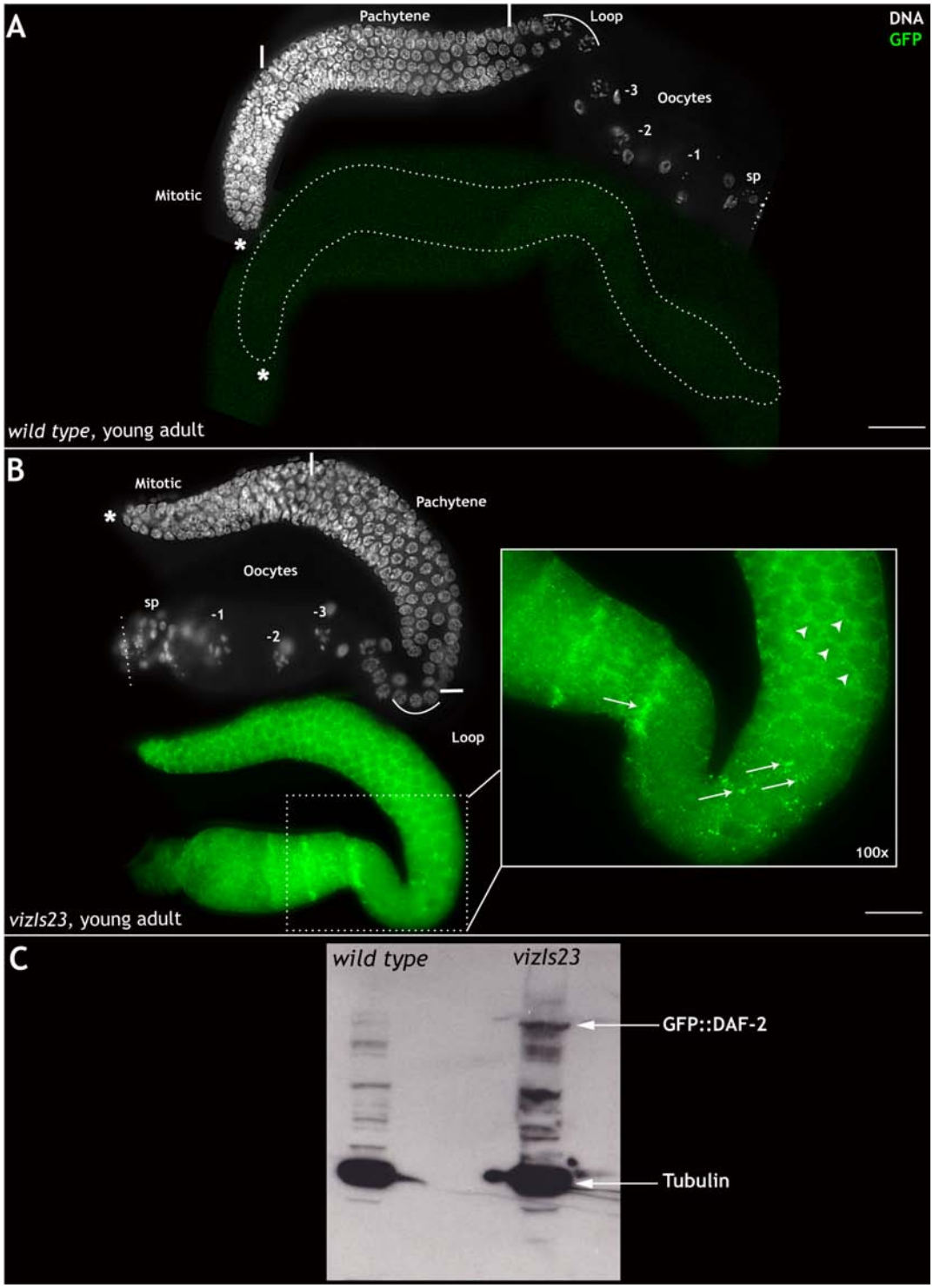

Figure S5, related to Figure 7

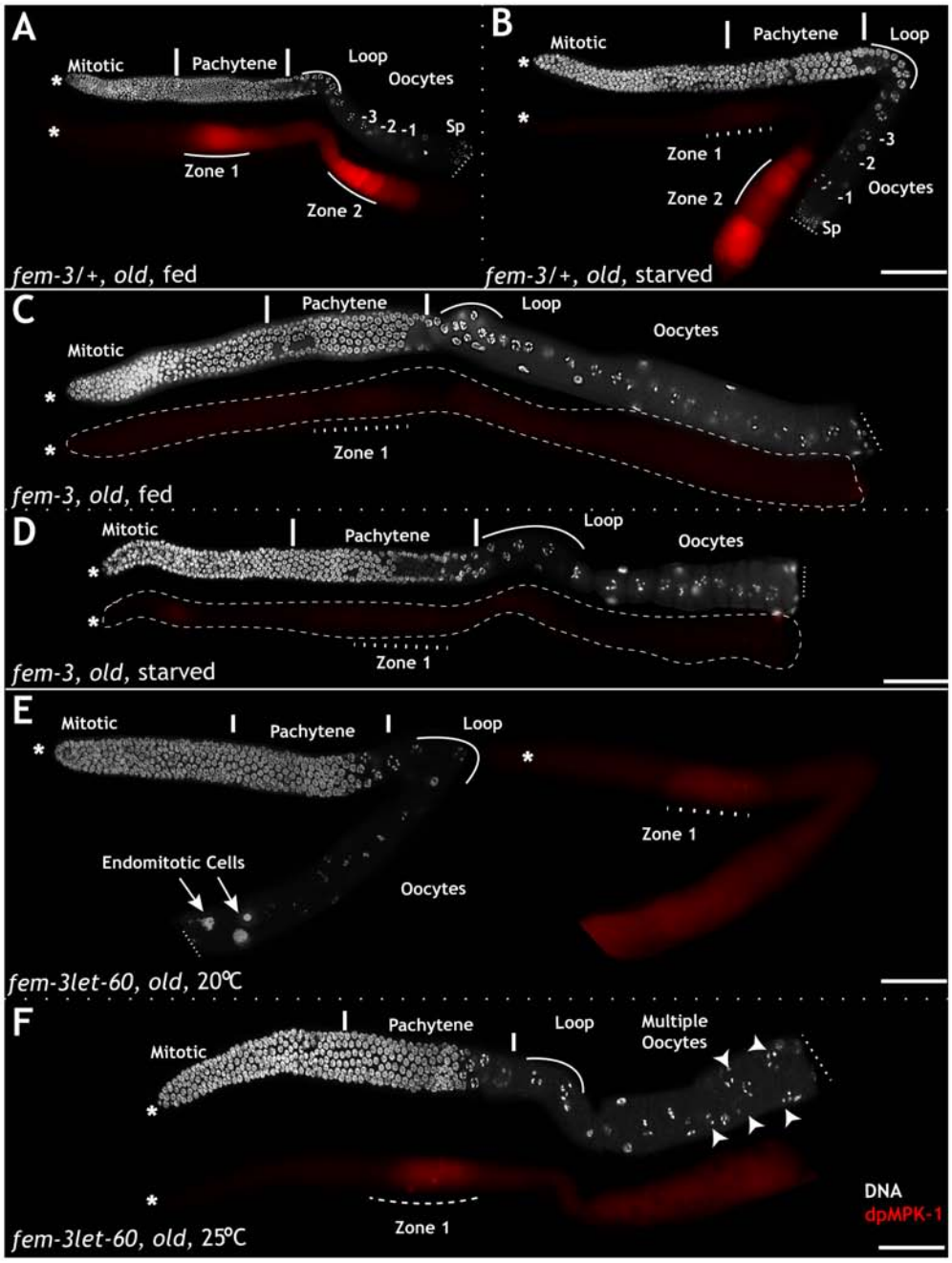

SUPPLEMENTAL FIGURE LEGENDS:

Figure S1, related to Figure 1: *daf-2* Insulin like receptor regulates MPK-1 activation and germ line development.

Dissected adult (24 hours past L4) hermaphrodite germ lines with mitotic cells on the left (*) and growing oocytes on the right stained with active MPK-1 (red) and DNA (DAPI, white). **A**: Germ lines obtained from *let-23(n1045)* loss-of-function animals exhibit wild type MPK-1 activation in zones 1 and 2 as well as normal germ line development. **B**: Germ lines obtained from *rrf-1;egl-15* RNAi animals exhibit normal germ line development as well as wild type zone 1 and 2 MPK-1 activation. We performed RNAi analysis of *egl-15* in *rrf-1* mutant animals because *egl-15* mutant animals are larval lethal. **C**: Quantitative RT PCR analysis performed on dissected germ lines obtained from *egl-15* RNAi and *gfp* RNAi in *rrf-1* animals, shows that *egl-15* RNA was reduced in the germ line upon RNAi treatment. *act-1* was used to normalize the templates and *gpd-3* was used as an internal control for the qRT-PCR analysis. Error bars depict standard deviation. For each immunofluorescence experiment over 50 germ lines were assayed. The experiment was repeated twice. qRT-PCR experiment was performed with 200 germ lines each. **D-E**: Germ lines obtained from wild type and *daf-2(e1370)* animals grown on 1mM DA at 25^{o}C (restrictive temperature for *daf-2*). **D**: Upon DA treatment, wild type germ lines appear normal with oocytes growing in a linear order (-1, -2). **E**: Germ lines obtained from *daf-2* animals cultured on DA reveal severe pachytene disorganization, pachytene progression and oocyte disorganization defects, as seen in *mpk-1* null animals. **F-G**: Germ line-specific depletion of *daf-2* RNAi results in loss of active MPK-1 in both zones 1 and 2, increased germ cell apoptosis (arrow heads), pachytene progression (PP) and disorganized oocytes. *gfp* RNAi is used as a control in the experiment. The DA experiments were performed four times, and each time 10-15

germ lines were analyzed. The RNAi experiment was performed twice and over 60 germ lines assayed each time. Scale bar: 20μm

H-O: Quantitative pixel intensity measure using Image J from four independent wild type and *daf-2* mutant germ lines maintained on food at 25^{o}C. **H-M**: Graphs showing pixel intensity of dpMPK-1 in zone 1 from four independent germ lines obtained from wild type animals. **N-O**: Graphs showing pixel intensity of dpMPK-1 in zone 1 from four independent germ lines from *daf-2* mutant animals. X-axis shows the position of different germ cells along the length of the germ line and Y-axis shows the dpMPK-1 accumulation as pixels. While each germ line has a different absolute level of dpMPK-1 accumulation in zones 1, the trend is always the same: high in zone 1 in wild type germ lines and low in zone 1 from *daf-2* mutant germ lines.

Figure S2, related to Figure 2: Nutrient sensing and not caloric restriction regulates MPK-1 activation in zone 1.

A-D: Dissected adult (24 hours past L4) hermaphrodite germ lines from wild type animals displaying mitotic cells on the left (*) and growing oocytes on the right, under fed (A) and starved conditions of 1 hour (B), 4 hours (C) and 6 hours (D). Staining reveals MPK-1 activation (red) and DNA (DAPI, white). **B**: MPK-1 activation is progressively lost from zone 1 starting at one hour of starvation. **C**: By 4 hours of starvation oocyte disorganization phenotypes are visible (arrows). **D**: By 6 hours of starvation, pachytene progression and large oocyte formation is visible similar to defects from loss of *daf-2* gene activity. The starvation time course was repeated five times and each time 10-15 germ lines were assayed.

E-G: Dissected adult (24 hours past L4) germ lines from wild type (E), *daf-2* mutant animals (F), or *eat-2* mutant animals (G), stained with REC-8 in green to mark mitotic population, active

MPK-1 (red) and DNA (DAPI, white). The germ lines are oriented left to right from mitotic cells (*) to growing oocytes. **E**: Germ lines obtained from wild type animals reveal normal zone 1 and 2 MPK-1 activation, as well as normal proliferation in the mitotic zone (REC-8, green). **F**: Reduction in *daf-2* function at 25^{o}C reveals MPK-1 activation and oocyte production (1 oocyte in *daf-2* mutant *vs* 5 in wild type). **G**: Germ lines obtained from *eat-2(ad465)* maintained on food exhibits wild type dpMPK-1 accumulation in zones 1 and 2, as well as oocyte production. Each experiment was performed three times and 20-25 germ lines analyzed. Scale bar: 20μm

Figure S3, related to Figure 3: *age-1* and *akt-1* do not regulate dpMPK-1 in zone 1 or oocyte development.

A-C: Dissected adult (24 hours past L4) germ lines from indicated genotypes displaying mitotic cells on the left (*) and growing oocytes on the right stained with active MPK-1 (red), REC-8 (green) and DNA (DAPI, white). Germ lines obtained from *rrf-1* animals upon RNAi treatment of *gfp* (A), *akt-1* (B) or *age-1* (C) reveal normal zone 1 and 2 MPK-1 activation, as well as normal germ line proliferation and oocyte production. **D**: Quantitative RT PCR analysis performed on dissected germ lines obtained from *akt-1* and *age-1* RNAi in *rrf-1* animals, shows that *akt-1* and *age-1* are reduced in the germ line upon RNAi treatment. *act-1* was used to normalize the templates and *gpd-3* was used as an internal control for the qRT-PCR analysis. Error bars depict standard deviation. The RNAi experiment was performed four times, with qRT-PCR analysis in parallel. For immunofluorescence analysis each time 20-25 germ lines were assayed. For the qRT-PCR analysis 200 germ lines were used per experiment. Scale bar: 20μm.

Figure S4, related to Figure 4: DAF-2::GFP accumulates in cytoplasm, plasma membrane and cytoplasmic vesicles in the germ line.

A-B: Germ lines obtained from wild type and *vizIs23* overexpression animals stained with DNA (DAPI, white) and GFP (green) reveal no GFP staining in wild type animals. In *vizIs23*, DAF-2::GFP, GFP staining reveals accumulation in three compartments in the germ line: plasma membrane (arrow heads, inset), cytoplasm and cytoplasmic vesicles (arrows, inset). **C**: Western blot analysis of wild type and *vizIs23* extracts with anti-GFP and anti-Tubulin antibodies. *vizIs23* extracts reveal a band at ~200kDa showing GFP::DAF-2. Tubulin on the same blot controls for lysate loading.

Figure S5, related to Figure 7: Old female germ lines containing stock pile of oocytes are resistant to effects of starvation.

Dissected adult *C. elegans* germ lines from wild type animals displaying mitotic cells on the left (*) and growing oocytes on the right from old females (C, D) or old *let-60(ga89gf);fem-3* (E, F) with either fed or starved conditions. DAPI (white) marks DNA and active MPK-1 is visualized in red. **A-B**: Germ lines obtained from age-matched *fem-3* heterozygous animals display wild type MPK-1 activation on food, and down regulate zone 1 MPK-1 activation upon two hours of starvation (B). **C-D**: Germ lines obtained from old female mutants exhibit down regulation of zone 1 MPK-1 activation, and lack of zone 2 activation both on (C) and off food (D). The germ lines of old females contain 12-14 oocytes arrested at the end of meiosis I. Once the female animals have built a stockpile of oocytes that are arrested in Meiosis I, they down regulate oocyte production and MPK-1 activation (C). At this condition, when oocytes are no longer being produced, these germ lines are resistant to the effects of starvation (D). **E-F**: Germ lines

obtained from *let-60(ga89gf)* females exhibit mild activation of zone 1 MPK-1 activation with premature reentry into cell cycle in the arrested oocytes resulting in endomitosis (E, endomitotic oocytes) as well as production of multiple small oocytes (arrow heads, F), suggesting that failure to down regulate MPK-1 in these animals results in disruption of homeostasis and premature reentry into cell cycle. Scale bar= 20 μm

TABLE S1, related to Figure 1: Analysis of germ lines from RNAi mediated depletion of Receptor Tyrosine Kinases in *rrf-1*

Gene[#]	Germ line Phenotype^	N*
egl-15	WT	120
ver-1	WT	96
lin-18	WT	95
ddr-2	WT	100
cam-1	WT	80
rol-3	WT Pachytene progression	104
daf-2	Large oocytes Disorganized oocytes	110
let-23	WT	112
kin-15	WT	80
tkr-1	WT	95

vab-1 was not analyzed due to its previously characterized role in mediating MSP dependent MPK-1 signaling in zone 2 and not 1 of the germ line.

^The analysis was conducted with dpMPK-1 staining and analysis of germ line phenotypes by DAPI and membrane staining.

* Total number of germ lines analyzed is shown. The germ lines were from four independent experiments.

TABLE S2, related to Figure 1: Loss of *daf-2* function results in *mpk-1* like loss-of-function phenotypes

Phenotypes	Genotypes				N*
	WT (%)	*daf-2(e1370)* (%)	*daf-2(e1368)* (%)	*daf-2(m577)* (%)	
Pachytene Progression	0	92.2	90	57	150
Pachytene disorganization	0.8	91.7	90	57	150
Large oocytes	0	88	90	52	150
No oocytes	0	7.8	8	9	150
WT	99.2	0	2	34	150

* Total germ lines obtained from five independent experiments
All germ lines were analyzed 24 hours past L4
Germ line phenotypes were observed with DAPI (for DNA) and membrane staining.

SUPPLEMENTAL EXPERIMENTAL PROCEDURES

C. elegans Strains

Standard procedures for culture and genetic manipulation of *Caenorhabditis elegans* strains were followed with growth at 20˚C (Brenner, 1974; Sulston and Brenner, 1974), except when noted otherwise. The Bristol strain N2 was used as the wild type strain. The following mutants were used: LG I: *daf-16*(*mu86)*, *muIs61*[*daf16::GFP* (*pKL78*)+*rol-6*(*pRF4*), *daf-16*(*m26*)*, rrf-1*(*pk1417*). LGII: *let-23*(*n1045*). *eat-2(ad453)*, *eat-2(ad465)* LG III: *daf-2*(*e1370ts*)*, daf-2*(*m577ts*), *daf-2*(*e1368ts*)*, stIs11614*[*daf-16f::H1-mcherry+unc-119(+). , mpk-1*(*ga111ts*). LG IV: *let-60*(*ga89ts*), *fem-3*(*e1996)/nT1GFP*, *daf-18*(*ok480*). The following double mutants were generated: *rrf-1*(*pk1417*);*daf-2*(*e1370*)III, *rrf-1*(*pk1417*)I*;daf-18*(*ok480*)IV *daf-2*(*e1370ts*)*III*;*fem-3*(*e1996*)/*nT1GFPIV, daf-2*(*e1370ts*)*/hT2GFPIII*;*let-60*(*ga89ts*)*IV*, *unc-24fem-3*(*e1996*)*let-60*(*ga89ts*)*IV/nT1GFP*. *mpk-1*(*ga111ts*)*III;daf-18*(*ok480*)*IV*. *daf-16*(*m26*)*I;daf-2*(*e1370ts*)*III* was kindly provided by Dr. Danielle Garsin at the University of Texas Health Science Center at Houston School of Medicine. The strains used were provided by the *Caenorhabditis* Genetics Center.

Female experiments.

Young females were defined as 4 or 6 hours past L4 stage of development. *let-60(ga89gf)* females were shifted to the restrictive temperature of 25^{o}C for four hours (at 2 hours past L4). *daf-2* females were shifted to the restrictive temperature of 25^{o}C for six hours at L4.

Transgenic construction of GFP::DAF-2

To create a GFP::DAF-2 construct, the *daf-2* coding region from the start codon to the translation stop was amplified as one PCR product of 5.5 Kb with KOD polymerase (Novagen, Madison,

WI), using the following primers: 5′ region—atgaatattgtcagatgtcggagacgacac and 3′ region—tcagacaagtggatgatgctcattatcctc. The products were amplified as attB1 and attB2 products and recombined into the pDONR vector of the gateway system. The pDONR plasmid was then sequenced and recombined into the pID3.02 *pie-1* GFP plasmid containing the *unc-119* transformation marker. Microparticle bombardment was used to create low-copy integrated transgenic lines (Praitis et al., 2001) in *unc-119(ed3)* animals as described earlier. Wild type animals were individually cloned and assayed for integration of the transgene. Two integrated lines were obtained and named *vizIs22* and *vizIs23*. All further analysis was performed on *vizIs23 [$_p$pie-1::gfp::daf-2; unc-119 (+)]; unc-119(cd3)*, since it had the most homogeneous phenotype.

RNA interference analysis

daf-2, daf-16 and *egl-15* RNAi clones were generated by amplification of 1 KB of the open reading frame starting from ATG, and inserted into the pPD129.36 RNAi vector. The clones were sequence verified before analysis. *mpk-1* and *mek-2* RNAi clones were obtained from the Vidal RNAi library and sequence verified before analysis. RNAi analysis was performed as described earlier (Arur et al., 2011; Arur et al., 2009). *daf-2* and *daf-16* RNAi analysis was performed as an F1 analysis. *egl-15* RNAi led to early larval lethality and thus RNAi analysis was performed with L1 larvae grown on RNAi plates and analyzed 24 hours past L4 as P0's. All the RNAi's above were performed in the *rrf-1* background. RRF-1 is a soma specific RNA dependent RNA polymerase that is necessary for the RISC complex to function in the soma (Sijen et al., 2001). In the absence of *rrf-1*, RNAi is elicited in the germ line but not in most of the somatic tissues, thus the function of genes can be assayed during adult germ line

development. Similarly for *mpk-1* and *mek-2* RNAi, L1 *vizIs23* animals were grown on RNAi plates and analyzed 24 hours past L4.

Antibodies

The following antibodies were used: anti-MAP Kinase used at 1:200 (Clone MAPK-YT, Sigma, St. Louis, MO). Anti-PTC-1 used at 1:50 (gift from Dr. Patty Kuwabara, Cambridge University, UK), anti-SYN-4 used at 1:200 (gift from Dr. Michael Glotzer, University of Chicago, Chicago). anti-CeLMN used at 1:200 (gift from Dr. Kelly Liu, Columbia University). anti-REC8 used at 1:100 (Novus Biologicals, Littleton, CO). Secondary antibodies were donkey anti-mouse Alexa Fluor 594, goat anti-rabbit Alexa Fluor 488, and goat anti-rabbit Alexa Fluor 594, goat anti-guinea pig 488 (all obtained from Molecular Probes, Eugene, OR). All secondary antibodies were used at 1:400.

Image acquisition and processing

Each gonad was captured as a montage, with each image taken as a 0.15µ section. The focal plane was maintained throughout the experiment. Each image was captured with overlapping cell boundaries at 40x magnification. All images were taken on a Zeiss Axio Imager upright microscope by using AxioVs40 V4.8.2.0 microimaging software and a Zeiss Axio MRm camera. The montages were then assembled in Adobe Photoshop CS5.1 and processed identically.

Quantitative image analysis for dpMPK-1 levels in Image J

To obtain linear measurements of the pixel intensity for dpMPK-1 staining in zone 1, the dissections for all the genotypes were performed on the same day, and processed in parallel.

Images of all the genotypes were collected on the same day. The values for dpMPK-1 in zone 1 were recorded, and the same value was used to image all the genotypes in a given experiment. Setting the dpMPK-1 gain in zone 1 in wild type led to some saturation of signal in *let-60(ga89)* animals for Figure 6. To measure the actual pixel intensity of dpMPK-1 staining, the images were imported into Image J (http://rsb.info.nih.gov/ij/) as tiff files. The free hand tool was used and a line was drawn from the center of the germ line (DNA was used for orientation) from the distal end (marked with the *) to the end of the germ line and pixel intensity was quantified using "Plot Profile". The graphs were then exported as tif files and labeled for presentation.

Western Blot analysis

Wild type (N2), and *vizIs23* L4 hermaphrodites were hand picked (250 for each lane), grown for 24 hours and then harvested for western analysis as previously described (Lee et al., 2007). The extracts were resolved on 10% SDS-PAGE, transferred to PVDF membrane, and probed with antibodies to GFP (made in house). Western blots were developed using SuperSignal West Pico Chemiluminescent Substrate from (Pierce, Rockford, IL), on Kodak BioMax MS films.

Quantitative RT-RCR (qRT-PCR)

qRT-PCR was performed as described earlier (Joo et al., 2009). Total RNA was isolated from worms using miRNeasy Mini Kit (QIAGEN, Germantown, MD) and was reverse transcribed to cDNA using the iScript cDNA synthesis kit (BIO-RAD, Hercules, CA). qRT-PCR reaction was performed using the iTaq Universal SYBR Green Supermix (BIORAD) according to the manufacturer's instructions, on a CFX96 Real-Time PCR system (BIORAD). Relative expression rate (%) was determined using the ΔΔCt method, and an expression rate of the

reference gene *act-1* was used for normalization of the expression levels. *gpd-3* was used as an internal control in all the experiments. Each experiment was performed in triplicate.

Primer sequences used in the experiment for each gene are as below:

act-1 RT-F1: 5' acccaaatcatgttcgagaccttc
act-1 RT-R1: 5' catttcttgctcgaagtcgagggc
product size: 323bp

gpd-3 RT-F1: 5' tgacaacttcggaattattgagg
gpd-3 RT-R1: 5' acaacttgatcctcggtgtaagc
product size : 351bp

egl-15 RT-F1: 5' agtcaaacgacaacattgtattgtt
egl-15 RT-R1: 5' attagccaaaatattcggaacgata
product size: 333bp

akt-1 RT-F1: 5' gctcggtaaaggaacattcg
akt-1 RT-F1: 5' caatatcgcatcggtgaagg
product size: 344bp

age-1 RT-F1: 5' cgaaactccgaaatctctgc
age-1 RT-R1: 5' cttgctctgttttggtgtgc
product size: 343bp

SUPPLEMENTAL REFERENCES

Angelo, G., and Van Gilst, M.R. (2009). Starvation protects germline stem cells and extends reproductive longevity in C. elegans. Science *326*, 954-958.

Arur, S., Ohmachi, M., Berkseth, M., Nayak, S., Hansen, D., Zarkower, D., and Schedl, T. (2011). MPK-1 ERK controls membrane organization in C. elegans oogenesis via a sex-determination module. Developmental cell *20*, 677-688.

Arur, S., Ohmachi, M., Nayak, S., Hayes, M., Miranda, A., Hay, A., Golden, A., and Schedl, T. (2009). Multiple ERK substrates execute single biological processes in Caenorhabditis elegans germ-line development. Proc Natl Acad Sci U S A *106*, 4776-4781.

Brenner, S. (1974). The genetics of Caenorhabditis elegans. Genetics *77*, 71-94.

Joo, H.J., Yim, Y.H., Jeong, P.Y., Jin, Y.X., Lee, J.E., Kim, H., Jeong, S.K., Chitwood, D.J., and Paik, Y.K. (2009). Caenorhabditis elegans utilizes dauer pheromone biosynthesis to dispose of toxic peroxisomal fatty acids for cellular homoeostasis. Biochem J *422*, 61-71.

Lee, M.H., Ohmachi, M., Arur, S., Nayak, S., Francis, R., Church, D., Lambie, E., and Schedl, T. (2007). Multiple functions and dynamic activation of MPK-1 extracellular signal-regulated kinase signaling in Caenorhabditis elegans germline development. Genetics *177*, 2039-2062.

Praitis, V., Casey, E., Collar, D., and Austin, J. (2001). Creation of low-copy integrated transgenic lines in Caenorhabditis elegans. Genetics *157*, 1217-1226.

Sijen, T., Fleenor, J., Simmer, F., Thijssen, K.L., Parrish, S., Timmons, L., Plasterk, R.H., and Fire, A. (2001). On the role of RNA amplification in dsRNA-triggered gene silencing. Cell *107*, 465-476.

Sulston, J.E., and Brenner, S. (1974). The DNA of Caenorhabditis elegans. Genetics *77*, 95-104.